The Fate of Methylmercury Through Formation of Bismethylmercury Sulfide as an Intermediate in Mice

Yumi Abiko
University of Tsukuba
Yusuke Katayama
University of Tsukuba
Wenyang Zhao
National Institute for Materials Science
Sawako Horai
National Institute for Minamata Disease
Kenji Sakurai
National Institute for Materials Science
Yoshito Kumagai (yk-em-tu@md.tsukuba.ac.jp)
University of Tsukuba

Research Article

Keywords: Methylmercury, Bismethylmercury sulfide, Dimethylmercury, Reactive sulfur species

Posted Date: April 30th, 2021

DOI: https://doi.org/10.21203/rs.3.rs-454570/v1

The fate of methylmercury through formation of bismethylmercury sulfide as an intermediate in mice

Yumi Abiko[1], Yusuke Katayama[2], Wenyang Zhao[3,4], Sawako Horai[5], Kenji Sakurai[3,4], Yoshito Kumagai[1, 2, *]

[1] Faculty of Medicine, University of Tsukuba, Tsukuba, Ibaraki 305-8575, Japan

[2] Master's Program of Medical Sciences, Graduate School of Comprehensive Human Sciences, University of Tsukuba, Tsukuba, Ibaraki 305-8575, Japan

[3] Doctoral Program in Materials Science and Engineering, Graduate School of Pure and Applied Sciences, University of Tsukuba, Tsukuba, Ibaraki 305-0006, Japan

[4] National Institute for Materials Science, Tsukuba, Ibaraki 305-0047, Japan

[5] Environmental Health Section, Dept. Environment and Public Health, National Institute for Minamata Disease, Minamata, Kumamoto 867-0008, Japan

[*]Address correspondence to Yoshito Kumagai, Faculty of Medicine, University of Tsukuba, 1-1-1 Tennodai, Tsukuba, Ibaraki 305-8575, Japan; Tel and Fax, +81-29-853-3133; E-mail, yk-em-tu@md.tsukuba.ac.jp

Abstract

A previous study of ours indicated that methylmercury (MeHg) is biotransformed to bismethylmercury sulfide [$(MeHg)_2S$)] by interaction with reactive sulfur species (RSS) produced in the body. In the present study, we explored the transformation of MeHg to $(MeHg)_2S$ in the gut and the subsequent fate of $(MeHg)_2S$ *in vitro* and *in vivo*. An *ex vivo* experiment suggested the possibility of extracellular transformation of MeHg to $(MeHg)_2S$ in the distal colon, and accordingly, the sulfur adduct MeHg was detected in the intestinal content and feces of mice given MeHg, suggesting that $(MeHg)_2S$ is formed from reactions of MeHg with RSS in the gut. In a cell-free system, we found that $(MeHg)_2S$ spontaneously undergoes degradation in a time-dependent fashion, resulting in formation of mercury sulfide, as determined by X-ray diffraction, and dimethylmercury (DMeHg), as evaluated by gas chromatography/mass spectrometry. We also identified DMeHg in expiration after intraperitoneal administration of $(MeHg)_2S$ to mice. Our present study therefore identifies a new fate of MeHg through $(MeHg)_2S$ as an intermediate, which leads to conversion of volatile DMeHg in the body.

Keywords: Methylmercury; Bismethylmercury sulfide; Dimethylmercury; Reactive sulfur species.

Introduction

Mercury species are naturally occurring substances and industrially produced environmental contaminants, and their biogeochemical cycle is well known. For example, volatile mercury species such as Hg^0 or inorganic Hg^{2+} is deposited on soil and in water bodies by rainfall during volcanic activity. Inorganic mercury is methylated to yield methylmercury (MeHg) and then undergoes further methylation to form dimethylmercury (DMeHg) through nonenzymatic reactions and/or biotransformations in microbes[1]. MeHg in the environment can accumulate in fishes such as tuna (*Thunnus*) and others marine creature[1,2]. We are mainly exposed to MeHg through intake of contaminated foods that are health risks. Due to electrophilic nature of MeHg, this organomercury compound covalently modifies protein thiols, leading to the formation of MeHg-protein adducts, thereby changing protein functions[3,4]. We have previously found that a lower MeHg dose modifies Kelch-like ECH-associated protein 1 (Keap1) and phosphatase and tensin homolog deleted on chromosome ten (PTEN), leading to activation of the Keap1/nuclear factor E2 related factor 2 (Nrf2) pathway and PTEN/Akt signaling, which are related to detoxication of xenobiotics and cell survival, respectively, whereas MeHg at a high dose disrupts cellular homeostasis, resulting in cell death[5,6]. While unlike MeHg, DMeHg has little electrophilicity to modify protein thiols but shows high and delayed toxicity[7,8].

After being incorporated into the body, MeHg is effectively absorbed from the gastrointestinal tract and distributed through blood to various organs. Some MeHg in tissues interacts with small molecular nucleophiles, such as glutathione (GSH) produced by glutamate-cysteine ligase (GCL), in the absence and presence of GSH *S*-transferase (GST); these interactions are referred to as phase II reactions and result in the formation of GSH adducts, which are excreted into extracellular space through multidrug resistance-associated protein (MRP) in phase III reactions[9]. The series of reactions regulated by Nrf2 are considered a strategy to remove hydrophobic MeHg from cells (tissues) by conversion to a more hydrophilic GSH adduct (Figure 1) because this transcription factor cooperatively regulates the gene expression of GCL, GST and MRP[10,11]. While this polar GSH conjugate a detoxified metabolite[9,12], the Hg-S bond on MeHg–SG adduct is unstable[13,14]. Supporting this, a study of ours suggested that MeHg–SG adduct undergoes *S*-transmercuration with reactive CysSH residues on proteins, resulting in formation of protein-MeHg adducts[15], which is associated with the activation of redox signaling pathways and toxicity[3,4], as mentioned above. On the other hand, we previously identified bismethylmercury sulfide [methyl(methylmercuriosulfanyl)mercury; $(MeHg)_2S$] as a metabolite of MeHg from the liver of rats given MeHg and neuroblastoma SH-SY5Y cells exposed to MeHg[16]. Subsequent examination indicated that $(MeHg)_2S$ is formed by the interaction of MeHg with reactive sulfur species (RSS); these species exhibit high nucleophilicity[17,18] and include such compounds as GSH persulfide (GSSH) derived from CysSH persulfide (CysSSH) and hydrogen sulfide (H_2S) produced by transsulfuration or enzymatic activities such as cystathionine γ-lyase (CSE) activity[19] (see Figure 1). Although gut microbiota can produce H_2S[20-22], the transformation of MeHg to $(MeHg)_2S$ in gut is unknown. Unlike the MeHg-SG adduct, $(MeHg)_2S$ is unable to interact with protein thiols[16], suggesting that this sulfur adduct no longer has the covalent binding capability involved in MeHg toxicity. Nevertheless, the important thing is that $(MeHg)_2S$ is more hydrophobic than parent compound MeHg. We therefore hypothesized that there is a system that excretes the sulfur adduct of MeHg to outside the body. In the present study, we explored 1) the biotransformation of MeHg to $(MeHg)_2S$ in gut and 2) the fate of $(MeHg)_2S$ *in vitro* and *in vivo*.

Results

Ex vivo and *in vivo* studies on the biotransformation of MeHg

Incubation of MeHg (200 μM) in the mouse distal colon but not in the duodenum with the colon's natural content (Figure 2A and 2B) for 30 min under aerobic conditions produced $(MeHg)_2S$, which was observed as a peak with a retention time of 10–14 min containing Hg by HPLC/AAS[19]. While $(MeHg)_2S$ was not detected during incubation of MeHg when the distal colon was washed with saline (Figure 2C), incubation of MeHg with even the content alone produced $(MeHg)_2S$ (Figure 2D). MeHg (10 mg/kg) was orally injected into mice, and $(MeHg)_2S$ formation in the gut was analyzed. As shown in Figure 2E–G, $(MeHg)_2S$ was detected in the distal colon content and fecal sample but not in the duodenum content. These results suggest that fecal excretion of $(MeHg)_2S$ is, at least partially, attributable to the formation of $(MeHg)_2S$ from MeHg by RSS, such as H_2S produced by the distal colon microbiota. Such a formation of $(MeHg)_2S$ from MeHg was also seen in the rectal content of another mammal, Javan mongoose (supplemental Figure S1).

Product analysis during spontaneous degradation of $(MeHg)_2S$

We tested the stability of $(MeHg)_2S$ at 25°C in 50 mM potassium phosphate buffer (KPi, pH 7.5) for 7 days. $(MeHg)_2S$ in the sample, as detected by high-performance liquid chromatography (HPLC)/atomic absorption spectrophotometry (AAS), was gradually degraded to 17.8% of the starting material, while MeHg was fairly stable under these conditions (supplemental Figure S2). We separated organic Hg species from the solution by liquid-liquid extraction with benzene and water and found that the Hg level in the benzene layer after 7 days was decreased to approximately 45.2% of the value at day 0, whereas the Hg level in the water layer increased in a time-dependent manner (Figure 3A). In a separate experiment, $(MeHg)_2S$ was also incubated with mouse liver supernatant centrifuged at 9,000 *g*. Although 72.2% of $(MeHg)_2S$ in 50 mM KPi buffer remained after one day, $(MeHg)_2S$ in the 9,000 *g* supernatant markedly declined to 20.8% (Figure 3B). This suggests that enzymes and/or low-molecular-weight components participate in $(MeHg)_2S$ decomposition. Notably, the material balance of Hg levels was incomplete under these conditions (Figure 3A), suggesting that unknown decomposition products seem to be volatile substances. To confirm this possibility, we collected unknown compounds from the head space of a sample tube containing $(MeHg)_2S$ by using XAD-4 resin for 3 h. Gas chromatography/mass spectrometry (GC/MS) revealed that a product derived from $(MeHg)_2S$ with a retention time of 2.5 min had m/z = 202 (^{202}Hg) (Figure 3E), which is identical to that of authentic dimethylmercury (DMeHg) analyzed by GC/MS (Figure 3C). In addition, the spectrum of the unknown product showing the parent ion (m/z = 232) and the fragment ions (m/z = 217, 202, and 15) (Figure 3F) were almost the same as that of authentic DMeHg (Figure 3E).

Moreover, we also collected black particles in the aqueous phase of the sample after incubation for 7 days, and the crystal structures were analyzed by X-ray diffraction (XRD). As shown in Figure 3G, the XRD pattern of the present black particles was nearly identical to that of authentic black β-HgS, which has a cubic structure (space group $F\bar{4}3m$, a = 0.58537 nm, ICDD PDF card 01-089-0432[23]). The four strongest peaks, at 26.34 deg, 43.72 deg, 51.76 deg, and 30.52 deg, were 111, 220, 311, and 200 reflections, respectively. A series of small peaks at 54.24 deg, 63.60 deg, 70.04 deg, 72.10 deg, 80.30 deg, 86.32 deg, 96.32 deg, 102.26 deg, 104.38 deg, and 112.80 deg were observed for 222, 400, 331, 420, 422, 511, 440, 531, 442, and 620 reflections, respectively[23]. One might find three or four small additional peaks between 20 deg and 30 deg in the XRD

patterns of the obtained black particles and authentic β-HgS (Figures 3G and 3H). As discussed in supplemental Figure S3, all such XRD peaks were well explained by considering the second phase, α-HgS, which has a hexagonal structure (space group $P3_221$, a = 0.41495 nm, c = 0.9497 nm, ICDD PDF card 00-042-1408[24]). In contrast, in Figure 3H, the XRD pattern of the present black particles was clearly different from that of $(MeHg)_2S$ itself, as the strongest peak from $(MeHg)_2S$, at 9.00 deg (corresponding to 0.983 nm interplanar spacing), vanished completely. This clearly demonstrates that the original $(MeHg)_2S$ had decomposed and that inorganic crystal of β-HgS was formed.

Detection of CH_4 during decomposition of DMeHg *in vitro*

Because it is suggested that DMeHg is unstable under acidic conditions[25,26], we incubated DMeHg or MeHg in 0.5 N HCl solution and analyzed the decomposition products. A peak with a retention time of 1.79 min, corresponding to methane (CH_4) (supplemental Figure S4A and S4B) on GC/MS, was detected in the head space of DMeHg but not MeHg at 3 h and 4 days of incubation (supplemental Figure S4C–S4G). This observation was in agreement with previous findings[26]. Under the same conditions, a product with a similar EI-MS fragmentation pattern to MeHgCl was also observed in the DMeHg solution (supplemental Figure S5A and 5B), and the peak containing Hg with the same retention time as authentic MeHg was detected by HPLC/AAS (supplemental Figure S5C and S5D). We also analyzed DMeHg dissolved in methanol by EI-MS and observed DMeHg, but the MeHg level was negligible (supplemental Figure S5E). These results suggest that DMeHg decomposed into CH_4 and MeHg in aqueous solution.

Identification of DMeHg from the exhaled breath of mice

Since DMeHg is a volatile material with a high vapor pressure (8.8 kPa at 20°C, reference from ICSC), we confirmed whether DMeHg derived from $(MeHg)_2S$ was distributed in the lung and then exhaled outside of the body. To address this issue, DMeHg (0.1 mmol/kg) was intraperitoneally injected into mice, and then the exhalation was collected for 3 h. As shown in Figure 4A and 4B, the collected sample peak with a retention time of 2.5 min was detected with an ion trace at m/z = 202 (^{202}Hg) and the spectrum pattern corresponded to authentic DMeHg (Figures 3C, 3D, 4A, and 4B). The samples collected 3 h following intraperitoneal administration of 0.01 mmol/kg $(MeHg)_2S$ or MeHg exhibited almost the same patterns as authentic DMeHg in GC/MS (Figure 4C and 4D, supplemental Figure S6).

Discussion

In the present study, we identified DMeHg as a decomposition product of $(MeHg)_2S$ derived from MeHg *in vitro* and *in vivo*. It was also shown that HgS was formed during the decomposition of $(MeHg)_2S$. In nonbiological samples, Craig and Bartlett previously observed biphasic decay of MeHg in the presence of H_2S in an aqueous reaction mixture; the first, rapid decay and second, slow decay were probably due to the formation of $(MeHg)_2S$, which is a somewhat water-insoluble material, and evolution of DMeHg from the reaction mixture, respectively[27], supporting the results of our cell-free study. A series of experiments led them to mention that H_2S generated in sediments may accelerate the transformation of MeHg to volatile DMeHg, which moves to the atmosphere[27-29]. Although as far as we know, there is no report regarding the biotransformation of $(MeHg)_2S$ to DMeHg in mammals, the present study indicates that $(MeHg)_2S$ biologically

produced from MeHg is a key intermediate in the production of DMeHg, which is released from the lungs in mice (Figures 4 and 5). Such $(MeHg)_2S$ degradation was facilitated by the addition of supernatant of mouse liver spun at 9,000 *g*, suggesting that unidentified enzymes and/or low-molecular-weight components contribute, at least in part, to the decomposition of $(MeHg)_2S$.

We initially reported that $(MeHg)_2S$ was formed during interactions with RSS, such as H_2S produced by cystathionine β-synthase (CBS)[16]. However, a subsequent study indicated that CBS and CSE catalyze the transformation of cystine to CysSSH, which interacts with GSH, forming GSSH and H_2S based on an equilibrium reaction among them[17]. In addition, we found that $(MeHg)_2S$ is formed with not only H_2S but also GSSH, GSSSG and the synthetic polysulfide Na_2S_4 during reaction with MeHg[19]. We have recently shown that there are phytochemical components containing RSS that form $(MeHg)_2S$ from MeHg in garlic[30]. We therefore speculate that simultaneous intake of fish such as tuna accumulating MeHg with garlic would potentially bring about increased formation of $(MeHg)_2S$ and concomitant production of DMeHg; as a result, accumulation of MeHg in the body may be repressed compared to the accumulation for intake without garlic. Further study is required to elucidate this possibility *in vivo*.

In addition to various enzymes (e.g., CBS and CSE) in organs, H_2S is produced by numerous gut microbes such as *Clostridium*, *Desulfovibrio*, *Escherichia*, *Klebsiella*, *Salmonella*, *Streptococcus*, and *Enterobacter*[20-22]. Although the gastrointestinal tract absorbs approximately 90% of MeHg[31], we assumed that whether MeHg reacts with H_2S or compounds with sulfane sulfur to form $(MeHg)_2S$ derived from the bacterial system in the mouse intestine. Herein, we show for the first time that $(MeHg)_2S$ is produced in the mouse distal colon but not in the duodenum with its contents and that the components in the distal colon react with MeHg to yield $(MeHg)_2S$ (Figure 2A–D). We also detected $(MeHg)_2S$ in the distal colon content and in mouse feces following MeHg administration (Figure 2E–G). LC/MS analysis indicated that relatively high levels of H_2S and minimal levels of CysSSH and GSSH were observed in the mouse intestine (Akiyama M et al., unpublished observation). Hence, it seems likely that the formation of $(MeHg)_2S$ in distal colon content and substantial excretion of this sulfur adduct in mice are attributable to gut microbe-dependent H_2S rather than CysSSH/GSSH extracellularly produced in the content of the mouse intestine. In the present study, we also detected $(MeHg)_2S$ from the rectal content of the wild small Indian mongoose (*Herpestes auropunctatus*), which has a relatively high level of total Hg in its tissues[32], that did not undergo artificial exposure to MeHg (supplemental Figure S1), suggesting that $(MeHg)_2S$ formation is due to a biotransformation mediated by gut microbe-dependent H_2S in the mongoose.

The causative agent of Minamata disease is MeHg, which is accidentally formed during the production of acetaldehyde in chemical factories. Nevertheless, a current topic is that HgS was identified in Cat 717 given industrial waste from Minamata in 1959 and that such inorganic mercury formation might be associated with α-mercuri-acetaldehyde ($CHOCH_2Hg$) rather than MeHg[33]. James et al. thermodynamically postulated that H_2S detected in the cat sample would be formed from α-bis-mercuri-acetaldehyde sulfide $[(CHOCH_2Hg)_2S]$ as an intermediate and that interaction of 2 moles of $CHOCH_2Hg$–cysteine adduct with H_2O is required for production of $(CHOCH_2Hg)_2S$[33]. However, the cleavage of C-S bond is fairly hard because the bond energy of the bond (259 kJ/mol) is relatively high. Importantly, however, is that $(CHOCH_2Hg)_2S$ and $(MeHg)_2S$ are structurally similar to each other, with different alkyl mercury groups cross-linked with sulfur atoms as shown in Supplemental Figure S7. In the present study, we showed that $(MeHg)_2S$ produced during interactions of

MeHg with RSS was not stable and thus underwent spontaneous decomposition, yielding DMeHg and H_2S. We therefore propose the alternative that $(CHOCH_2Hg)_2S$ is formed by reactions of $CHOCH_2Hg$ with RSS but not cysteine, if any is present *in vivo*, and then spontaneous decomposition occurs, leading to the formation of HgS and α-bis-mercuri-acetaldehyde $[(CHOCH_2)_2Hg]$ (supplemental Fig. S7).

According to the thermodynamically favored reaction mechanism[33] based on a reaction of $(CHOCH_2)_2Hg$ with H_2O, we incubated DMeHg with H_2O and found that methane (CH_4) and MeHg were formed from DMeHg under acidic conditions (Figure S4 and S5), suggesting that sulfur adducts of MeHg and $CHOCH_2Hg$ are critical precursors for 1) excretion from the body through formation of volatile DMeHg and its structurally related species $(CHOCH_2)_2Hg$ and 2) substantial preservation of these parent substances in the body by recycling of MeHg and $CHOCH_2Hg$ (Supplemental Fig. S7A). In the present study, HgS was also identified by XRD during spontaneous degradation of $(MeHg)_2S$, suggesting that HgS is the counterpart for DMeHg, although we did not examine the exact stoichiometry of $(MeHg)_2S$, and that these products formed in the study. Since HgS is an insoluble nanoparticle, the simple question of how this particle is stored or excreted out of the body should be addressed in the near future.

Methods

Materials and methods

Sigma-Aldrich (St. Louis, MO, USA) supplied MeHgCl (98% purity) and DMeHg (95% purity). Mercury standard solution, formic acid and methanol were obtained from Nacalai Tesque Inc. (Kyoto, Japan). Na_2S and XAD-4 were purchased from FUJIFILM Wako Pure Chemical Co. (Osaka, Japan) and ACROS Organics (Fair Lawn, NJ, USA), respectively. All other reagents used were of the highest purity available. $(MeHg)_2S$ was synthesized as previously described[16].

Animal experiments

All protocols for animal experiments, which were carried out in compliance with the ARRIVE guidelines, were approved by the University of Tsukuba Animal Care and Use Committee and followed the committee's guidelines for alleviating suffering. C57BL/6J 8-week-old female mice (Clea Japan, Tokyo, Japan) were fasted for 12 h before treatment with compounds, and all experiments with exposure to chemicals were performed with a single administration.

After euthanasia, the liver and intestine and their contents were extirpated for each experiment. The liver was homogenized in a 4× tissue volume of 50 mM KPi (pH 7.4), followed by centrifugation at 9,000 *g* for 10 min. MeHg (100 μM) was incubated in the liver supernatant centrifuged at 9,000 *g* (2 mg/mL) or in 50 mM KPi (pH 7.5) for 0–7 days at 37°C, and liquid-liquid extraction was performed to determine organic and/or inorganic Hg content by AAS (MA-3000; Nihon Instruments, Osaka, Japan). MeHg (200 μM in saline-5% methanol) was incubated in the mouse distal colon or duodenum with content or in the distal colon, which was washed with saline, for 30 min at room temperature. The distal colon (10 mg) was incubated with MeHg (200 μM) for 30 min at 25°C.

For HPLC/AAS analysis of $(MeHg)_2S$ in intestinal content or feces, mice were orally administered mercury compounds dissolved in saline. $(MeHg)_2S$ in fecal samples from mice given 10 mg/kg MeHg for 18-42 h was extracted by 50% methanol-10% formic acid. After centrifugation (13,000 *g*, 4°C), the samples were analyzed

by HPLC/AAS as described below.

To detect DMeHg from expiration, MeHgCl, DMeHg, or $(MeHg)_2S$ (0.1 mmol/kg) dissolved in corn oil was intraperitoneally injected into mice, and then the expiration was aspirated by pumping (50 mL/min) through a mask connected to an XAD-4 (500 mg) column for 3 h. XAD-4 was set on both sides (air in/out) of the mask to avoid contamination with mercury species from the environment. Absorbed chemicals were extracted by 1 mL of acetone and analyzed by GC/MS (GCMS-QP2020, Shimadzu, Kyoto, Japan).

Analysis of MeHg and $(MeHg)_2S$ by HPLC/AAS

MeHg and $(MeHg)_2S$ were detected fractions with retention times of approximately 3–5 min and 10–15 min, respectively, as previously described[16,19]. Briefly, samples were subjected to HPLC equipped with a Zorbax Eclipse XDB-C_{18} column (50 mm long, 2.1 mm i.d., 5 μm particle size; Agilent Technologies, Santa Clara, CA, USA). The mobile phase was 10% methanol-0.1% formic acid (the flow rate was 0.5 mL/min), and the mercury concentrations in the eluate fractions were determined using a direct thermal decomposition mercury analyzer with an AAS detector (MA-3000). A mercury standard solution diluted in 100 mg/L cysteine solution was used to prepare a standard curve for AAS.

Detection of organic and inorganic Hg from $(MeHg)_2S$

$(MeHg)_2S$ (100 μM) in 50 mM KPi (pH 7.5) was incubated for 0–7 days at 37°C. An aliquot of the sample (500 μL) was mixed with 100 μL of 6 N HCl and 600 μL of benzene and stirred for 5 min. After centrifugation (13,000 *g*, 5 min) of the mixture, a benzene layer was collected, and then 600 μL of benzene was added to the water layer. The extraction process was repeated 4 times. The Hg content was measured by AAS in the collected benzene layer and water layer, which was neutralized by the addition of 1.71 N NaOH (500 μL).

Determination of insoluble mercury

$(MeHg)_2S$ (10 mM) in 50 mM KPi (pH 7.5) was stirred for 7 days at room temperature and then filtered. The residue was washed with 20 mL of pure water and 20 mL of methanol, dried using an aspirator, suspended in pure water and benzene and stirred for 5 min. After centrifugation, Hg in the benzene layer was determined by AAS. The process was repeated until the Hg content in the benzene layer was less than 10 ng. The solvents were removed, and then the residue was washed with 10 mL of methanol 3 times and dried by an aspirator. To determine the crystal structure of the compound, powder XRD experiments (Rigaku Ultima-III, Cu Kα, 40 kV –30 mA, θ/2θ scanning, angular step 0.02 deg, 3 sec accumulation per step) were carried out.

Detection of volatile Hg by GC/MS

Volatile Hg compounds were collected by XAD-4, and then the absorbed chemicals were extracted by 1 mL of acetone and analyzed by GC/MS. The samples were separated by an InertCap 5MS/Sil column (30 m long, 0.25 mm i.d., 0.25 μm df; GL Sciences, Tokyo, Japan) that was maintained at 40°C, and He gas (≥ 99.99995% purity) was used as the carrier gas. The temperature was set as follows: 40°C for 5 min; a linear increase to 150°C (6°C/min); hold at 150°C for 5 min; an increase to 200°C over 1 min. The eluted compounds were then transferred to the EI source (70 eV) of the system, and the control and analyses were performed using GCMSsolution ver 4.44 (Shimadzu)*. *Unfortunately, we were not able to determine DMeHg

quantitatively using GC/MS because of its high vapor pressure.

Statistical analysis

Each experiment was repeated at least three times, and representative data are shown. Statistical significance was assessed by the differences in a population mean test, followed by the Welch test, and $P < 0.05$ was considered significant.

Acknowledgments

This work was supported in part by Grants-in-Aid for Scientific Research (18H05293 to Y. Kumagai) from the Ministry of Education, Culture, Sports, Science and Technology of Japan and by Research funding to Y.A. from the Urakami Foundation for Food and Food Culture Promotion. We thank Masahiro Akiyama, who kept and cared for the mice until the experiments.

Author contributions

Y.A. performed HPLC/AAS and GC/MS, discussed the results and contributed to writing the manuscript. Y. Katayama performed AAS analysis following liquid-liquid extraction and GC/MS. K.S. and W. Z contributed to XRD analysis. S.H. captured the mongoose and prepared the samples. Y. Kumagai supervised and coordinated the research.

Additional Information

Competing financial interests

The authors declare no competing interests.

Corresponding author

Correspondence should be addressed to Yoshito Kumagai.

Data Availability

All data generated or analysed during this study are included in this published article and its Supplementary Information files.

References

1 Hintelmann, H. Organomercurials. Their formation and pathways in the environment. *Met. Ions Life Sci.* **7**, 365-401, doi:10.1039/BK9781847551771-00365 (2010).

2 Grandjean, P., Satoh, H., Murata, K. & Eto, K. Adverse effects of methylmercury: environmental health research implications. *Environ. Health Perspect.* **118**, 1137-1145, doi:10.1289/ehp.0901757 (2010).

3 Kanda, H., Shinkai, Y. & Kumagai, Y. S-mercuration of cellular proteins by methylmercury and its toxicological implications. *J. Toxicol. Sci.* **39**, 687-700 (2014).

4 Simpson, R. B. Association Constants of Methylmercury with Sulfhydryl and Other Bases. *J. Am. Chem. Soc.* **83**, 4711-&, doi:DOI 10.1021/ja01484a005 (1961).

5 Toyama, T. *et al.* Cytoprotective role of Nrf2/Keap1 system in methylmercury toxicity. *Biochem. Biophys. Res. Commun.* **363**, 645-650, doi:10.1016/j.bbrc.2007.09.017 (2007).

6 Unoki, T. *et al.* Methylmercury, an environmental electrophile capable of activation and disruption of the Akt/CREB/Bcl-2 signal transduction pathway in SH-SY5Y cells. *Sci. Rep.* **6**, 28944, doi:10.1038/srep28944 (2016).

7 Joshi, D., Mittal, D. K., Shukla, S. & Srivastav, A. K. Therapeutic potential of N-acetyl cysteine with antioxidants (Zn and Se) supplementation against dimethylmercury toxicity in male albino rats. *Exp. Toxicol. Pathol.* **64**, 103-108, doi:10.1016/j.etp.2010.07.001 (2012).

8 Nierenberg, D. W. *et al.* Delayed cerebellar disease and death after accidental exposure to dimethylmercury. *N. Engl. J. Med.* **338**, 1672-1676, doi:10.1056/NEJM199806043382305 (1998).

9 Ballatori, N. Transport of toxic metals by molecular mimicry. *Environ. Health Perspect.* **110 Suppl 5**, 689-694 (2002).

10 Itoh, K. *et al.* Keap1 regulates both cytoplasmic-nuclear shuttling and degradation of Nrf2 in response to electrophiles. *Genes Cells* **8**, 379-391 (2003).

11 Mahaffey, C. M. *et al.* Multidrug-resistant protein-3 gene regulation by the transcription factor Nrf2 in human bronchial epithelial and non-small-cell lung carcinoma. *Free Radic. Biol. Med.* **46**, 1650-1657, doi:10.1016/j.freeradbiomed.2009.03.023 (2009).

12 Ketterer, B., Coles, B. & Meyer, D. J. The role of glutathione in detoxication. *Environ. Health Perspect.* **49**, 59-69, doi:10.1289/ehp.834959 (1983).

13 Rabenstein, D. L., Reid, R. S. & Isab, A. A. H nmr study of the effectiveness of various thiols for removal of methylmercury from hemolyzed erythrocytes. *J. Inorg. Biochem.* **18**, 241-251 (1983).

14 Rabenstein, D. L., Arnold, A. P. & Guy, R. D. 1H-NMR study of the removal of methylmercury from intact erythrocytes by sulfhydryl compounds. *J. Inorg. Biochem.* **28**, 279-287 (1986).

15 Yoshida, E., Abiko, Y. & Kumagai, Y. Glutathione adduct of methylmercury activates the Keap1-Nrf2 pathway in SH-SY5Y cells. *Chem. Res. Toxicol.* **27**, 1780-1786, doi:10.1021/tx5002332 (2014).

16 Yoshida, E. *et al.* Detoxification of methylmercury by hydrogen sulfide-producing enzyme in Mammalian cells. *Chem. Res. Toxicol.* **24**, 1633-1635, doi:10.1021/tx200394g (2011).

17 Ida, T. *et al.* Reactive cysteine persulfides and S-polythiolation regulate oxidative stress and redox signaling. *Proc. Natl. Acad. Sci. U. S. A.* **111**, 7606-7611, doi:10.1073/pnas.1321232111 (2014).

18 Ono, K. *et al.* Redox chemistry and chemical biology of H2S, hydropersulfides, and derived species: implications of their possible biological activity and utility. *Free Radic. Biol. Med.* **77**, 82-94, doi:10.1016/j.freeradbiomed.2014.09.007 (2014).

19 Abiko, Y. *et al.* Involvement of reactive persulfides in biological bismethylmercury sulfide formation. *Chem. Res. Toxicol.* **28**, 1301-1306, doi:10.1021/acs.chemrestox.5b00101 (2015).

20 Tomasova, L. *et al.* Intracolonic hydrogen sulfide lowers blood pressure in rats. *Nitric Oxide* **60**, 50-58, doi:10.1016/j.niox.2016.09.007 (2016).

21 Blachier, F., Beaumont, M. & Kim, E. Cysteine-derived hydrogen sulfide and gut health: a matter of endogenous or bacterial origin. *Curr. Opin. Clin. Nutr. Metab. Care* **22**, 68-75, doi:10.1097/MCO.0000000000000526 (2019).

22 Barton, L. L., Ritz, N. L., Fauque, G. D. & Lin, H. C. Sulfur Cycling and the Intestinal Microbiome.

Dig. Dis. Sci. **62**, 2241-2257, doi:10.1007/s10620-017-4689-5 (2017).

23 Rodic, D., Spasojevic, V., Bajorek, A. & Onnerud, P. Similarity of structure properties of Hg1-xMnxS and Cd1-xMnxS (structure properties of HgMnS and CdMnS). *J. Magn. Magn. Mater.* **152**, 159-164, doi:Doi 10.1016/0304-8853(95)00435-1 (1996).

24 Penak, V., McCarthy, G. & Bayliss, P. (ICDD, North Dakota State Univ., Fargo, North Dakota, USA., 1991).

25 Fagerstrom, T. & Jernelov, A. Some aspects of the quantitative ecology of mercury. *Water Res.* **6**, 1193-1202, doi:https://doi.org/10.1016/0043-1354(72)90019-X (1972).

26 Bytautas, L. Stability of Dimethylmercury and Related Mercury-containing Compounds with Respect to Selected Chemical Species Found in Aqueous Environment. *Croat. Chem. Acta.* **86**, 453-462, doi:10.5562/cca2314 (2013).

27 Craig, P. J. & Bartlett, P. D. Role of Hydrogen-Sulfide in Environmental Transport of Mercury. *Nature* **275**, 635-637, doi:DOI 10.1038/275635a0 (1978).

28 Jonsson, S., Mazrui, N. M. & Mason, R. P. Dimethylmercury Formation Mediated by Inorganic and Organic Reduced Sulfur Surfaces. *Sci. Rep.* **6**, 27958, doi:10.1038/srep27958 (2016).

29 Kanzler, C. R. *et al.* Emerging investigator series: methylmercury speciation and dimethylmercury production in sulfidic solutions. *Environ. Sci. Process. Impacts* **20**, 584-594, doi:10.1039/c7em00533d (2018).

30 Abiko, Y., Katayama, Y., Akiyama, M. & Kumagai, Y. Lipophilic compounds in garlic decrease the toxicity of methylmercury by forming sulfur adducts. *Food Chem. Toxicol.* **150**, 112061, doi:10.1016/j.fct.2021.112061 (2021).

31 Berlin, M., Zalups, K. R. & Fowler, A. B. in *Handbook on the Toxicology of Metals* (eds G. Nordberg, B. Fowler, & M. Nordberg) Ch. 46, 1013-1075 (Academic Press, 2015).

32 Horai, S. *et al.* Establishment of a primary hepatocyte culture from the small Indian mongoose (Herpestes auropunctatus) and distribution of mercury in liver tissue. *Ecotoxicology* **23**, 1681-1689, doi:10.1007/s10646-014-1307-6 (2014).

33 James, A. K. *et al.* Rethinking the Minamata Tragedy: What Mercury Species Was Really Responsible? *Environ. Sci. Technol.* **54**, 2726-2733, doi:10.1021/acs.est.9b06253 (2020).

Figure legends

Figure 1. Biotransformation of methylmercury in the body.

CSE, cystathionine γ-lyase, CySSH, cysteine persulfide; GCL, glutamate-cysteine ligase; GSH, glutathione; GS^-, deprotonated form of GSH; GST, GSH *S*-transferase; CH_3Hg-SG, methylmercury GSH adduct; MRP, multidrug resistance associated protein

Figure 2. Detection of bismethylmercury sulfide as a reaction product of methylmercury with intestinal content *in vitro* and *in vivo*.

Blue bars indicate $(MeHg)_2S$. MeHg (200 μM) was incubated in mouse (A) distal colon or (B) duodenum with content, (C) distal colon without content, or (D) 10 mg of the content for 30 min. After 18 h of a single treatment with MeHg (10 mg/kg, p.o.), (E) the distal colon and (F) the duodenum contents were collected. (G) The feces from mice given MeHg (10 mg/kg, p.o.) was collected after 18 h–42 h of exposure. The samples were analyzed by HPLC/AAS. Representative data are shown.

Figure 3. Detection of volatile and insoluble mercury compounds during incubation with bismethylmercury sulfide.

(A) $(MeHg)_2S$ was incubated for 0–7 days at 37°C. After liquid-liquid extraction, the benzene layer and the water layer were separately analyzed by AAS. Each value is the mean ± SE of three determinations. $*P < 0.01$ vs. 0 day. (B) $(MeHg)_2S$ was incubated in mouse liver supernatant (Liver) isolated by centrifugation at 9,000 *g* or in 50 mM KPi (pH 7.5) (Control) for 0–7 days at 37°C and detected by HPLC/AAS. Each value is the mean ± SE of three determinations. $*P < 0.01$ vs. 0 day. The head space of a sample tube containing $(MeHg)_2S$ was collected and analyzed by GC/MS. (C) Chromatogram of authentic DMeHg and (D) spectrum of the peak with a retention time of 2.5 min. (E) Chromatogram of the collected compounds and (F) spectrum of the peak with a retention time of 2.5 min. The residue after 7 days of incubation with $(MeHg)_2S$ was purified. (G, H) The decomposition product (reaction product), (G) authentic β-HgS, and (H) $(MeHg)_2S$ were analyzed by X-ray diffraction, and the spectra are shown.

Figure 4. GC/MS analysis of mouse expiration after treatment with dimethylmercury or bismethylmercury sulfide.

Chemicals in the expiration of mice given a single injection of (A and B) 0.1 mmol/kg DMeHg and (C and D) $(MeHg)_2S$ were analyzed by GC/MS. (A and C) Chromatogram of the collected compounds and (B and D) spectra of the peak with a retention time of 2.5 min. Representative data are shown.

Figure 5. Excretion of dimethylmercury through formation of bismethylmercury sulfide in mice.

DMeHg, dimethylmercury; MeHg, methylmercury; $(MeHg)_2S$, bismethylmercury sulfide. MeHg was transformed into $(MeHg)_2S$ via reaction with reactive sulfur species in tissue and intestine. A portion of intestinal $(MeHg)_2S$ might be absorbed into the body. $(MeHg)_2S$ slowly decomposed to HgS and DMeHg, which could be excreted from the body.

Figure 1

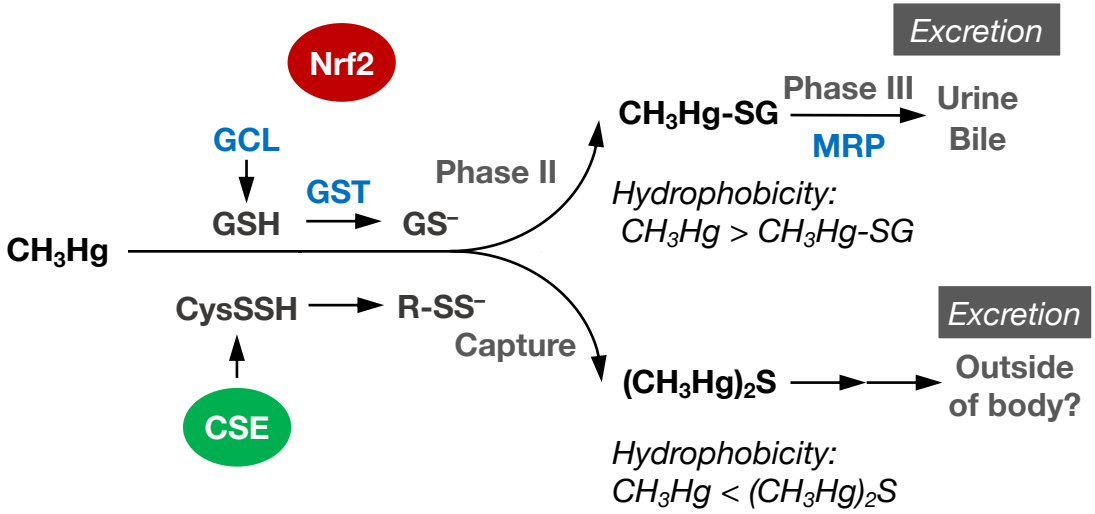
Nrf2
GCL
GST
GSH
GS⁻
Phase II
CH3Hg
CysSSH
R-SS⁻
Capture
CSE
Excretion
CH3Hg-SG
Phase III
MRP
Urine
Bile
Hydrophobicity:
CH3Hg > CH3Hg-SG
Excretion
(CH3Hg)2S
Outside
of body?
Hydrophobicity:
CH3Hg < (CH3Hg)2S

Figure 2

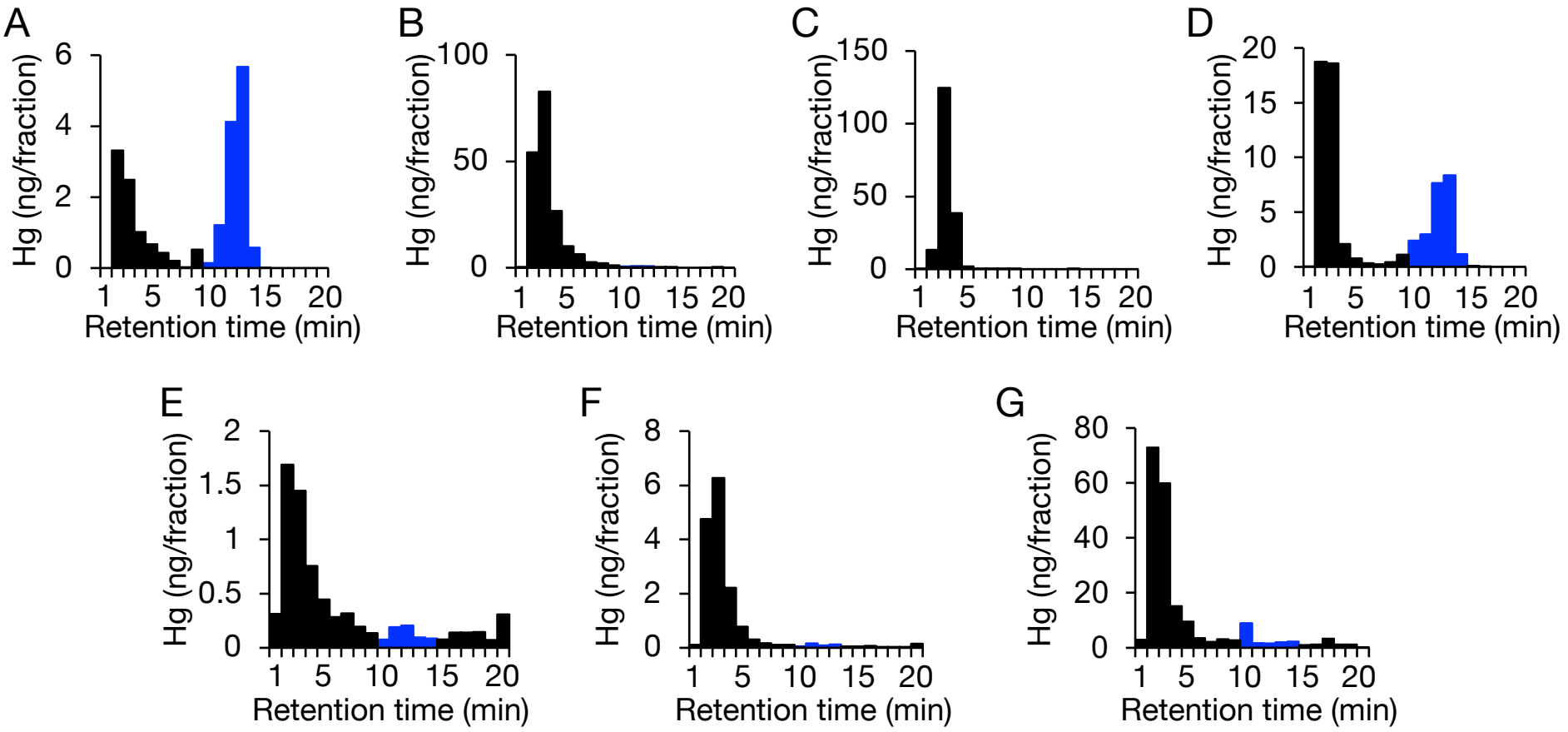
A
Hg (ng/fraction)
6
4
2
0
1 5 10 15 20
Retention time (min)
B
Hg (ng/fraction)
100
50
0
1 5 10 15 20
Retention time (min)
C
Hg (ng/fraction)
150
100
50
0
1 5 10 15 20
Retention time (min)
D
Hg (ng/fraction)
20
15
10
5
0
1 5 10 15 20
Retention time (min)
E
Hg (ng/fraction)
2
1.5
1
0.5
0
1 5 10 15 20
Retention time (min)
F
Hg (ng/fraction)
8
6
4
2
0
1 5 10 15 20
Retention time (min)
G
Hg (ng/fraction)
80
60
40
20
0
1 5 10 15 20
Retention time (min)

Figure 3

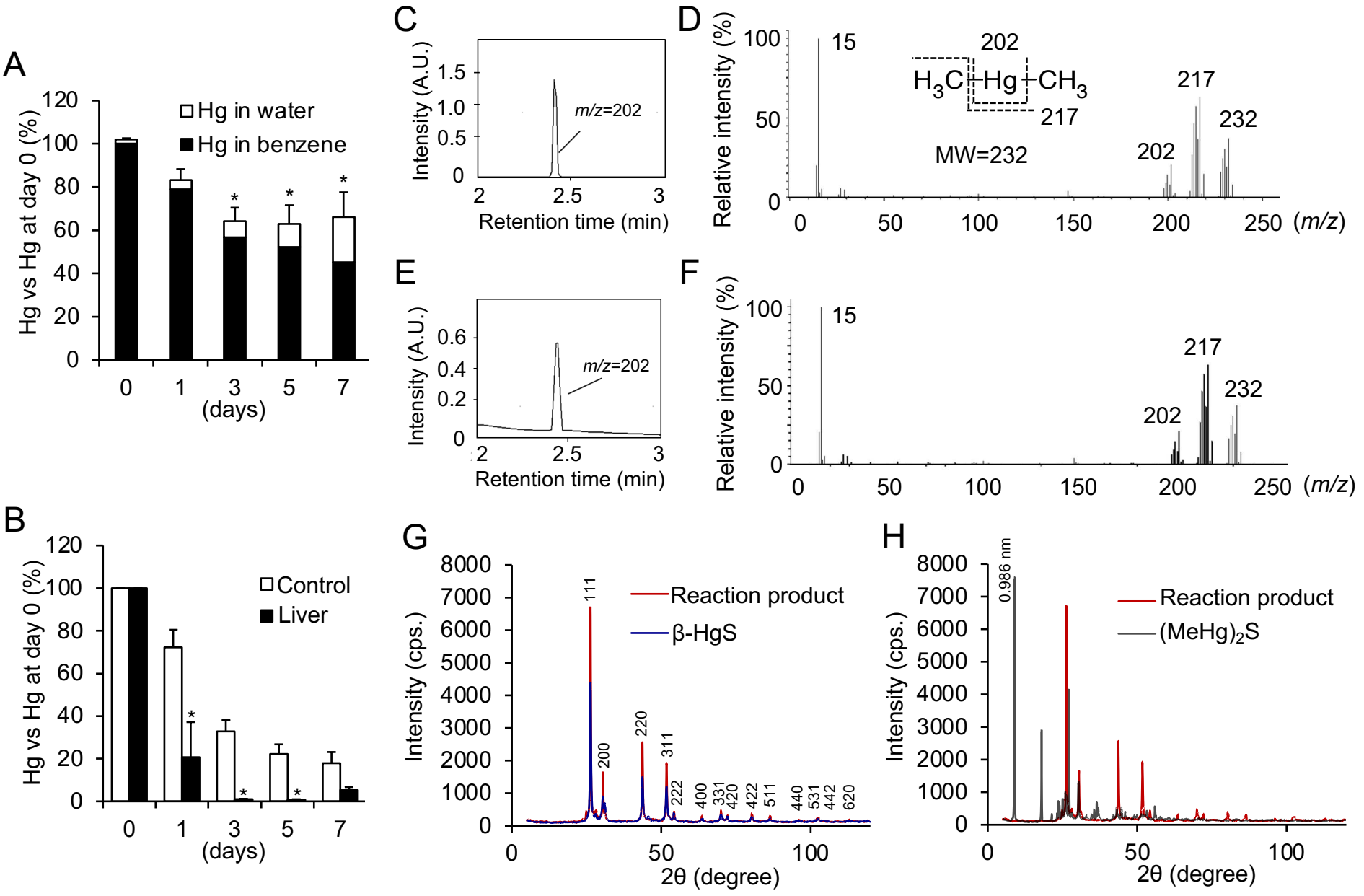
A
Hg vs Hg at day 0 (%)
Hg in water
Hg in benzene
(days)
B
Hg vs Hg at day 0 (%)
Control
Liver
(days)
C
Intensity (A.U.)
m/z=202
Retention time (min)
D
Relative intensity (%)
MW=232
(m/z)
E
Intensity (A.U.)
m/z=202
Retention time (min)
F
Relative intensity (%)
(m/z)
G
Intensity (cps.)
Reaction product
β-HgS
2θ (degree)
H
Intensity (cps.)
0.986 nm
Reaction product
(MeHg)2S
2θ (degree)

Figure 4

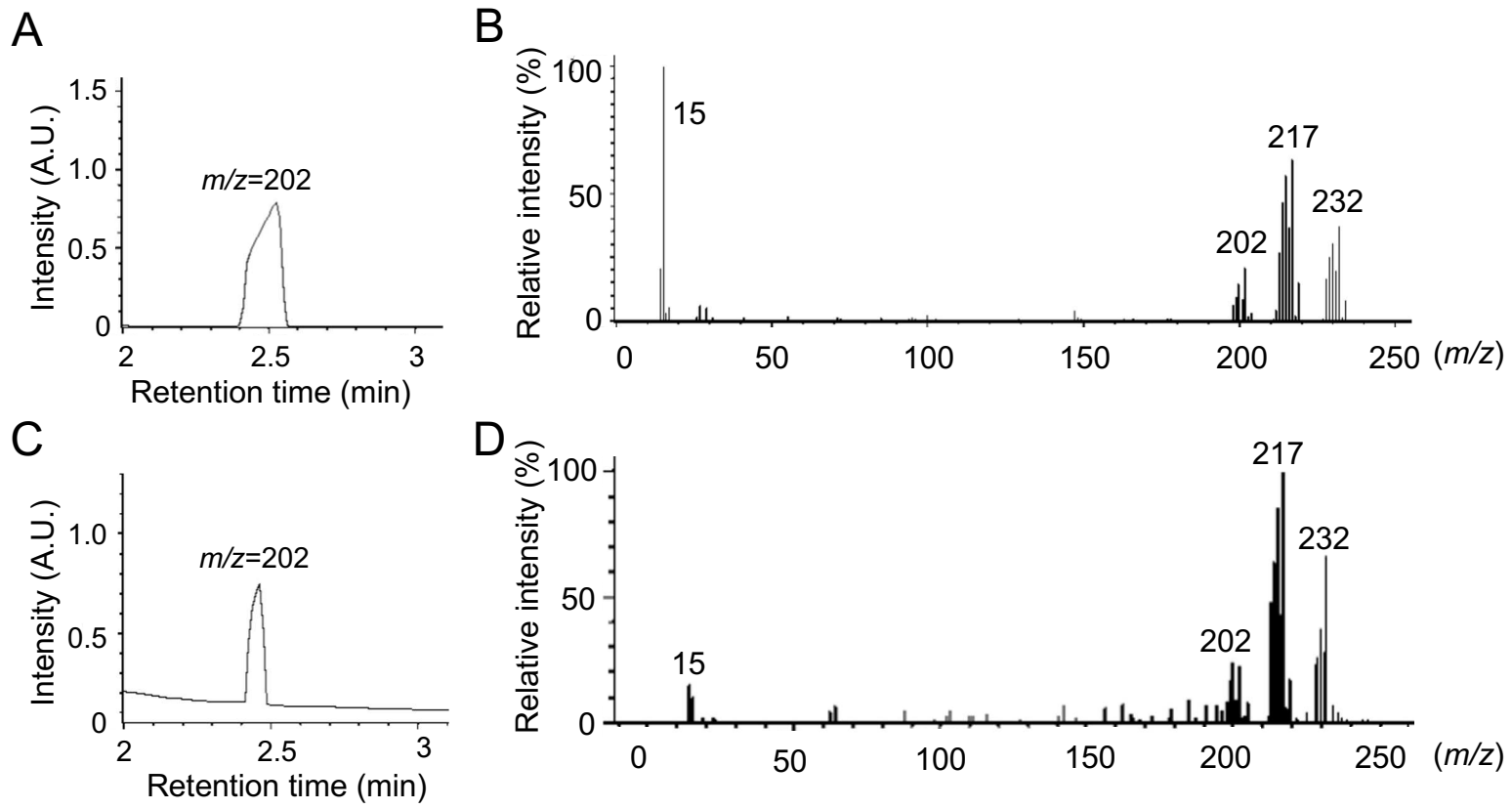
A
Intensity (A.U.)
1.5
1.0
0.5
0
m/z=202
2
2.5
3
Retention time (min)
B
Relative intensity (%)
100
50
0
15
202
217
232
0
50
100
150
200
250
(m/z)
C
Intensity (A.U.)
1.0
0.5
0
m/z=202
2
2.5
3
Retention time (min)
D
Relative intensity (%)
100
50
0
15
202
217
232
0
50
100
150
200
250
(m/z)

Figure 5

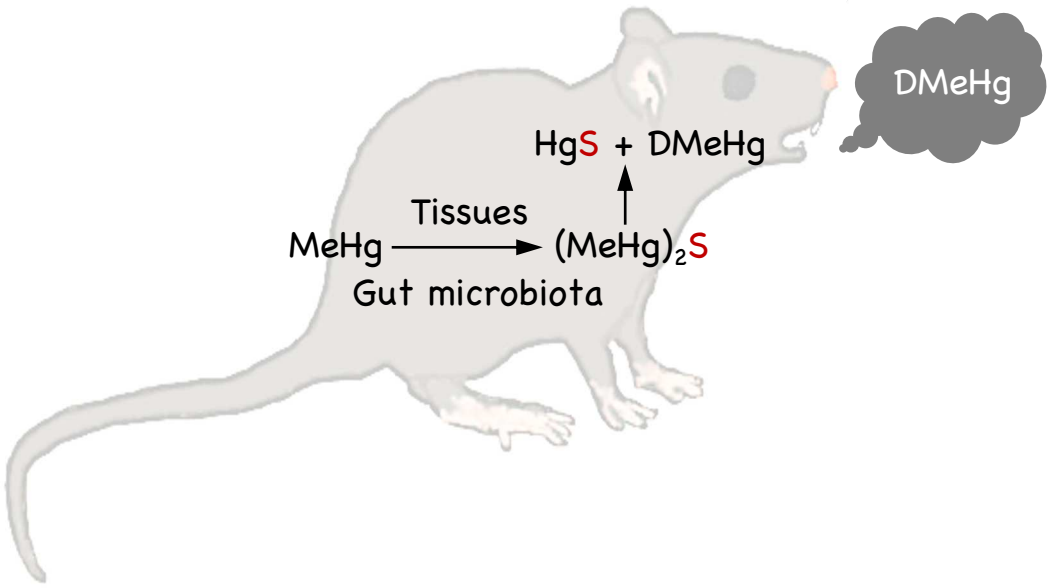

Figures

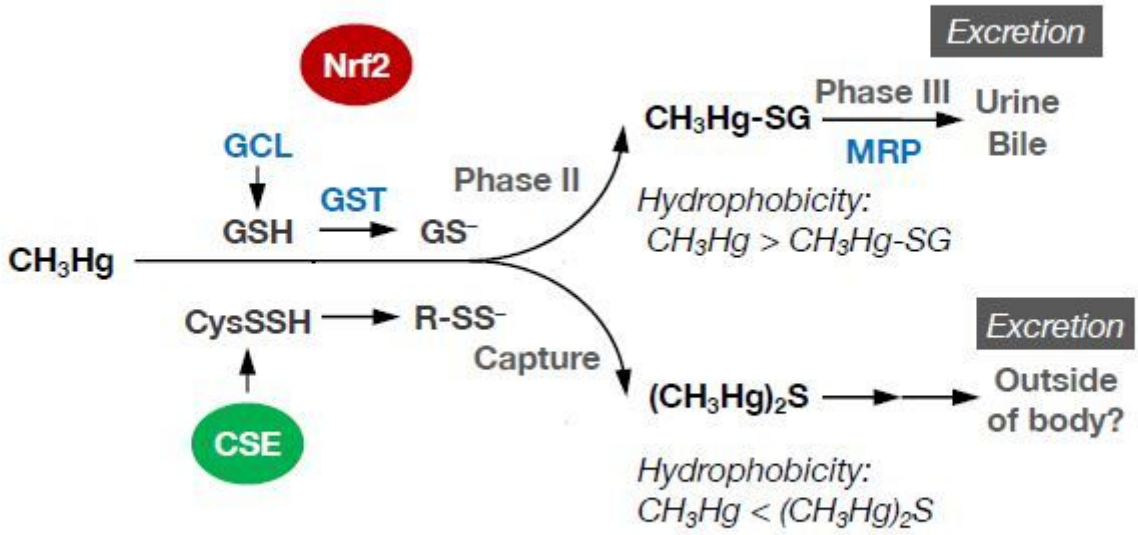

Figure 1

Biotransformation of methylmercury in the body. CSE, cystathionine g-lyase, CySSH, cysteine persulfide; GCL, glutamate-cysteine ligase; GSH, glutathione; GS–, deprotonated form of GSH; GST, GSH S-transferase; CH3Hg-SG, methylmercury GSH adduct; MRP, multidrug resistance associated protein

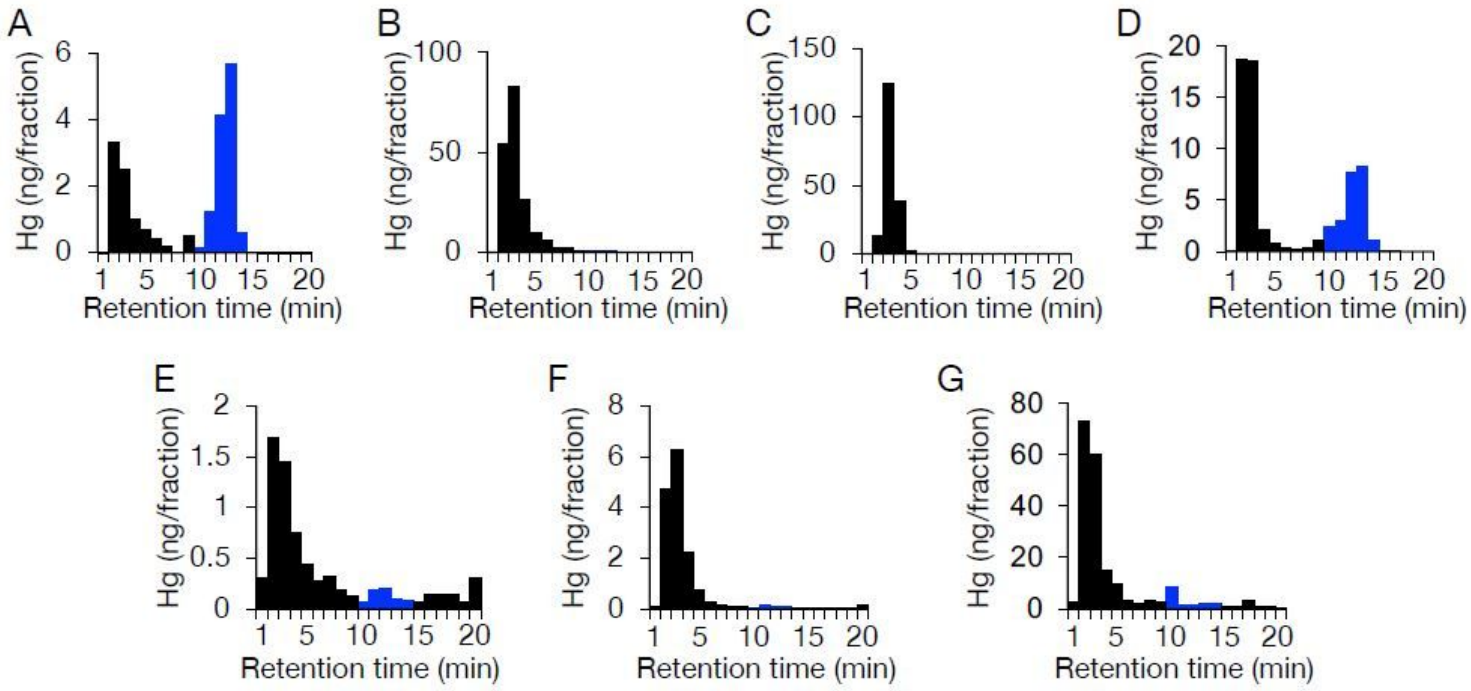

Figure 2

Detection of bismethylmercury sulfide as a reaction product of methylmercury with intestinal content in vitro and in vivo. Blue bars indicate (MeHg)2S. MeHg (200 μM) was incubated in mouse (A) distal colon or (B) duodenum with content, (C) distal colon without content, or (D) 10 mg of the content for 30 min. After 18 h of a single treatment with MeHg (10 mg/kg, p.o.), (E) the distal colon and (F) the duodenum contents were collected. (G) The feces from mice given MeHg (10 mg/kg, p.o.) was collected after 18 h–42 h of exposure. The samples were analyzed by HPLC/AAS. Representative data are shown.

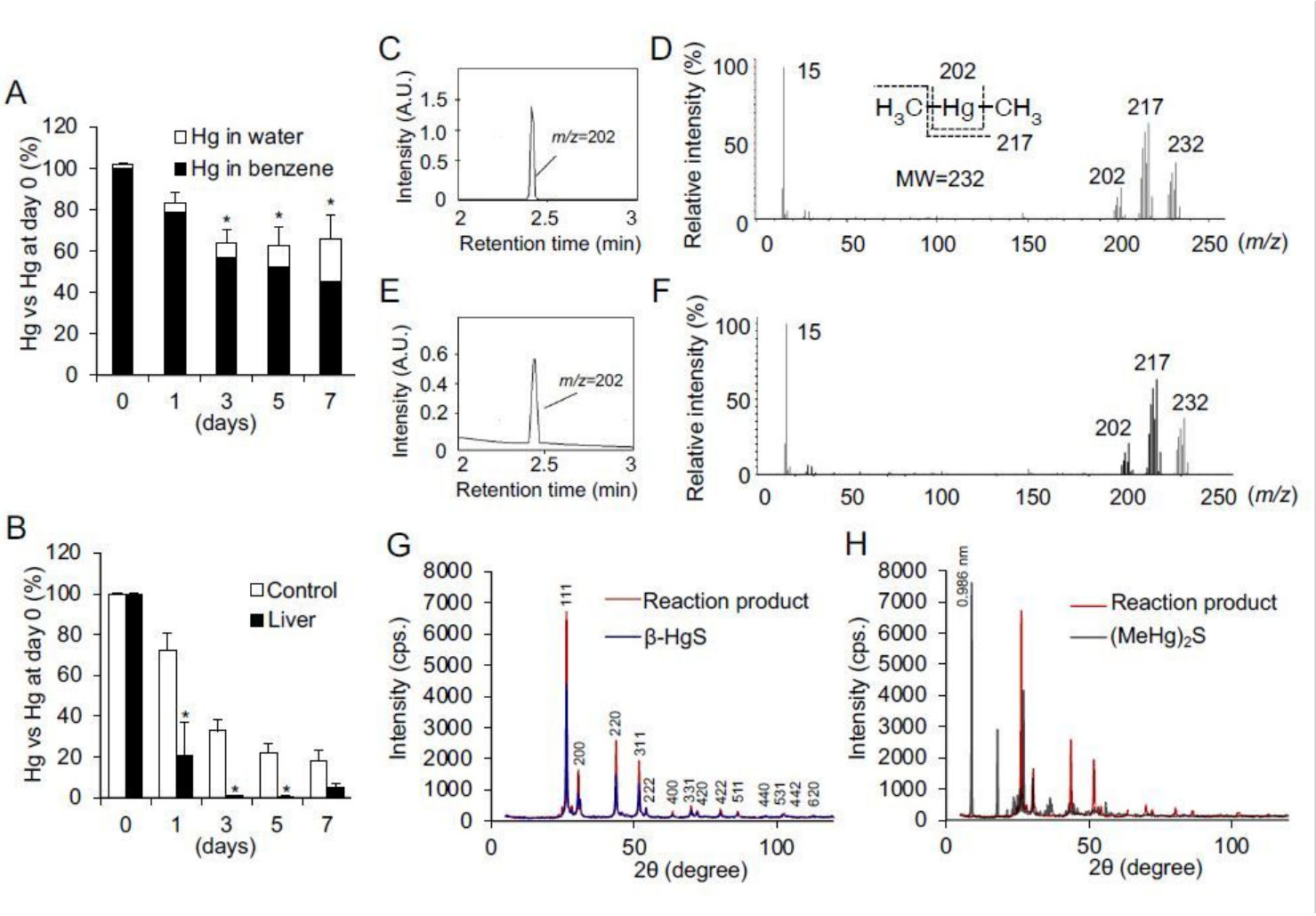

Figure 3

Detection of volatile and insoluble mercury compounds during incubation with bismethylmercury sulfide. (A) (MeHg)2S was incubated for 0–7 days at 37°C. After liquid-liquid extraction, the benzene layer and the water layer were separately analyzed by AAS. Each value is the mean ± SE of three determinations. *P < 0.01 vs. 0 day. (B) (MeHg)2S was incubated in mouse liver supernatant (Liver) isolated by centrifugation at 9,000 g or in 50 mM KPi (pH 7.5) (Control) for 0–7 days at 37°C and detected by HPLC/AAS. Each value is the mean ± SE of three determinations. *P < 0.01 vs. 0 day. The head space of a sample tube containing (MeHg)2S was collected and analyzed by GC/MS. (C) Chromatogram of authentic DMeHg and (D) spectrum of the peak with a retention time of 2.5 min. (E) Chromatogram of the collected compounds and (F) spectrum of the peak with a retention time of 2.5 min. The residue after 7 days of incubation with (MeHg)2S was purified. (G, H) The decomposition product (reaction product), (G) authentic b-HgS, and (H) (MeHg)2S were analyzed by X-ray diffraction, and the spectra are shown.

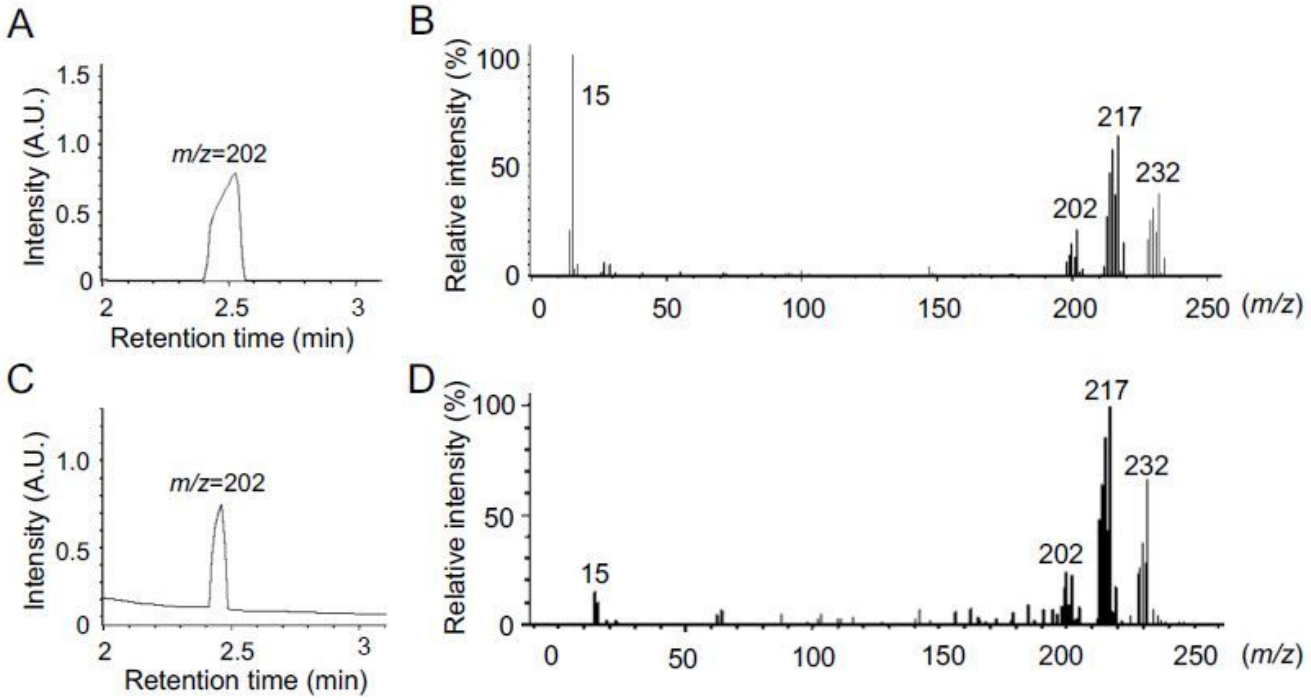

Figure 4

GC/MS analysis of mouse expiration after treatment with dimethylmercury or bismethylmercury sulfide. Chemicals in the expiration of mice given a single injection of (A and B) 0.1 mmol/kg DMeHg and (C and D) (MeHg)2S were analyzed by GC/MS. (A and C) Chromatogram of the collected compounds and (B and D) spectra of the peak with a retention time of 2.5 min. Representative data are shown.

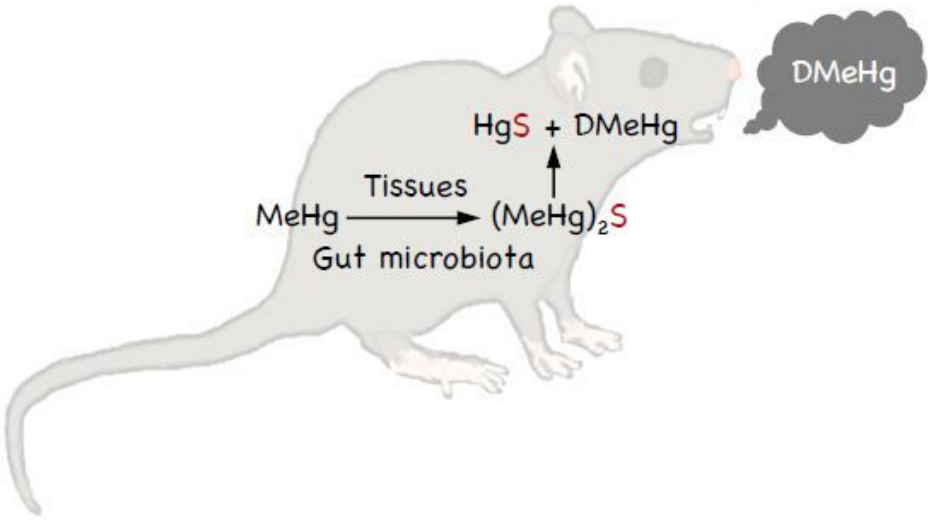

Figure 5

Excretion of dimethylmercury through formation of bismethylmercury sulfide in mice. DMeHg, dimethylmercury; MeHg, methylmercury; (MeHg)2S, bismethylmercury sulfide. MeHg was transformed into (MeHg)2S via reaction with reactive sulfur species in tissue and intestine. A portion of intestinal (MeHg)2S might be absorbed into the body. (MeHg)2S slowly decomposed to HgS and DMeHg, which could be excreted from the body.

Supplementary Files

This is a list of supplementary files associated with this preprint. Click to download.

- SupplementalmaterialsSciRepDiMeHgsubmit.pdf